electronics

Article

An Analytical Solution of the Multiple Scattering from a Buried Medium Coated Conducting Sphere

Chuan Yin, Liangjie Wu, Pengquan Zhang * and Youlin Geng *

Institute of Antennas and Microwaves, Hangzhou Dianzi University, Hangzhou 310018, China; yinc@hdu.edu.cn (C.Y.); 192040089@hdu.edu.cn (L.W.)
* Correspondence: zpq@hdu.edu.cn (P.Z.); gengyl@hdu.edu.cn (Y.G.)

Abstract: Based on the image method and addition theorem of spherical vector wave functions, an analytical solution of the multiple scattering by a buried medium-coated conducting sphere is proposed in this paper. An iterative process to obtain the scattered electromagnetic field is discussed on the basis of the continuous boundary condition in the plane boundary, the medium inner and the outer surface of a coated conducting sphere, respectively. Applying an image method and the addition theorem of spherical vector wave functions, the scattering electromagnetic fields by the plane in a local coordinate system can be transformed into the globe coordinate, and they can be regarded as the next incident electromagnetic fields to the buried medium-coated conducting sphere. This process does not end until the scattering electrical field on the plane boundary is accurate enough. Numerical results are given and compared with commercial software FEKO, they coincide enough; the calculation times of the present method are very short compared to those of the software FEKO, and some discussion is given at the end of this paper.

Keywords: electromagnetic scattering; buried medium coated conducting sphere; plane wave expanded; recursive algorithm; addition theorem

check for updates

Citation: Yin, C.; Wu, L.; Zhang, P.; Geng, Y. An Analytical Solution of the Multiple Scattering from a Buried Medium Coated Conducting Sphere. *Electronics* **2022**, *11*, 1632. https://doi.org/10.3390/electronics11101632

Academic Editors: Raed A. Abd-Alhameed, Panayiotis Frangos, Seil Sautbekov, Sava Savov and Hristos T. Anastassiu

Received: 28 March 2022
Accepted: 16 May 2022
Published: 20 May 2022

1. Introduction

The study of isotropic spheres is inevitably associated with the classical Lorenz–Mie theory, also known as Mie scattering theory, which was proposed by Lorenz in 1898 and later refined by Mie in 1908 on the basis of a separation method in a spherical coordinate [1]. Since then, based on the Lorenz–Mie theory, some works have been published [2–17]. In [2], the radar cross section of a spherical target is discussed, and the theory that the radar cross section of an electrically large spherical target is twice the cross section of the sphere itself is explained in [3]. In [4], the scattering of multiple perfect electric conducting (PEC) spheres is studied by using the generalized Lorenz–Mie theorem and the vector translation addition theorem, an inhomogeneous elliptically polarized plane wave scattering by perfect conducting. Dielectric spheres in free space are also discussed in detail in [5], and the discussion can easily be applied to the case of lossy media. Some scholars have turned their attention to the problem of electromagnetic scattering characteristics of complex spherical targets after studying the scattering of a single-layer sphere by plane waves. The scattering characteristics of uniformly charged coated spheres were analyzed in [6], and the charges on the inner core and outer shell were numerically calculated, respectively, when the surface is charged, and the extinction efficiency is affected by the radius ratio of the two layers and the surface potential. The problem of electromagnetic scattering of multilayered spheres is discussed after studying the electromagnetic scattering of single and coated spheres in [7], the study of scattering by two PEC spheres in terms of translation addition theorem is derived in [8], and in [9], the generalized Lorenz–Mie theory for laser-beam scattering by a perfect electromagnetic conductor (PEMC) sphere is derived and some characterization of laser scattering by a PEMC sphere is given in detail. In addition to the above studies, the problem of spherical electromagnetic scattering in free space is also discussed in [10,11].

The research of electromagnetic scattering from buried spheres is more complex to analyze than that by spheres in free space [1–11], but good progress has still been made [12–18] since electromagnetic scattering from buried objects can be used in the area of the detection of tunnels, pipes and mines, geophysical prospection, microwave remote sensing, medical diagnosis (skin tumor detection), etc. In [12], a general full-wave analytical solution is given to solve the problem of electromagnetic scattering by a buried dielectric or metallic sphere. A hybrid Kirchhoff approximation and electric field integral equation is deployed in [13] to analyze the electromagnetic scattering. In the same year, the electromagnetic scattering by elliptically polarized plane waves on single-layer and concentric double-layer spheres were analyzed [14,15]. An analytical expression for the scattering coefficients of a buried dielectric sphere under a rough interface by combing the small perturbation method and the Mie theory are presented in [16]. On the basis of the addition formula of Bessel functions and the multiple reflection approach from a buried cylinder and a buried conductor cylinder [19] and spherical vector wave function addition theorem [20,21], a solution to the scattering by a buried sphere and two buried concentric spheres are obtained in [17,18].

On the basis of the new study on electromagnetic scattering by a buried sphere and two buried concentric spheres [17,18], a recursive algorithm to study the electromagnetic scattering of a buried medium-coated conducting sphere is derived; the same as in [18], this paper is the extension of reference [17]. First, the transmitted electromagnetic fields into the isotropic medium can be regarded as the first incident electromagnetic fields of the buried medium-coated conducting sphere when a plane wave propagates vertically from free space to an isotropic medium, and it can be expanded using spherical vector wave functions. Second, electromagnetic fields in medium-coated conducting spheres can be expanded as the addition of the first and second spherical vector wave functions in isotropic medium, and then, using the tangential continuous boundary conditions of electromagnetic fields on the inner and outer surface of the medium-coated conducting sphere, the expanded coefficients of scattering electromagnetic fields of the buried medium-coated conducting sphere in terms of spherical vector wave functions can be derived. Third, applying the image method [17,19] and the addition theorem of the spherical vector wave functions [20,21], the reflection electromagnetic fields in local coordinate system from the plane interface are derived, which are regarded as the second incident electromagnetic fields to the buried medium-coated conducting sphere. This process does not end until the electrical field in the plane boundary is accurate enough. Some numerical results are obtained and compared with those of the FEKO software, and they coincide very well.

2. Formulation

Consider the geometry depicted in Figure 1, which shows a coated sphere whose inner and outer radii of the medium-coated conducting sphere are r_1 and r_2. The origin of the coordinate system is in the center of the medium-coated conducting sphere in region 1. Throughout this paper, a time factor $e^{-i\omega t}$ is assumed and omitted, while ω is the angular frequency of the incident electromagnetic field.

A plane wave whose electric field amplitude is 1 propagates in the z-direction from region 0 to region 1, and the electric and magnetic fields of the incident electromagnetic field can be expressed as [17–19]:

$$\mathbf{E}_{i1} = \hat{x} e^{ik_0 z} \quad z < -d \tag{1}$$

$$\mathbf{H}_{i1} = \hat{y} \frac{1}{\eta_0} e^{ik_0 z} \quad z < -d \tag{2}$$

where k_0 and η_0 are the wave number and wave impedance in free space (region 0), respectively. The incident electromagnetic fields will produce reflected electromagnetic fields (in region 0) and transmitted electromagnetic fields (in region 1) at the plane $z = -d$, which can be expressed in the following [17–19]:

$$\mathbf{E}_{r1} = \hat{x}\, Re^{-ik_0 z} \quad z < -d \tag{3}$$

$$\mathbf{H}_{r1} = -\hat{y}\frac{1}{\eta_0} Re^{-ik_0 z} \quad z < -d \tag{4}$$

$$\mathbf{E}_{t1} = \hat{x}\, Te^{ik_1 z} \quad z > -d \tag{5}$$

$$\mathbf{H}_{t1} = \hat{y}\frac{1}{\eta_1} Te^{ik_1 z} \quad z > -d \tag{6}$$

where k_1 and η_1 are the wave number and wave impedance in region 1, respectively. In this discussion, transmitted electromagnetic fields are of interest, and T is the transmitted coefficient of the plane $z = -d$, which can be obtained by bringing Equations (1)–(6) into the tangential continuous boundary conditions of the electromagnetic field, and the transmitted coefficient T can be obtained [17–19]:

$$T = \frac{2\eta_1}{\eta_1 + \eta_0} e^{i(k_1 - k_0)d} \tag{7}$$

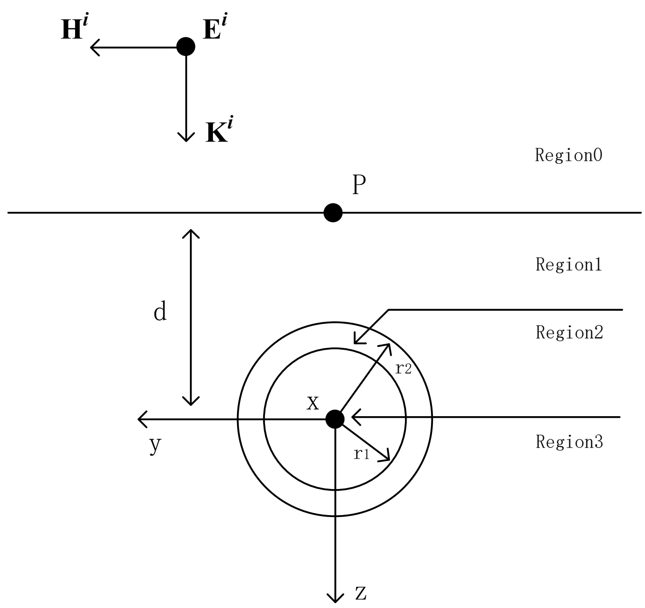

Figure 1. Geometric model of a buried medium-coated conducting sphere.

The transmitted electromagnetic fields $\mathbf{E}_{t1}$ and $\mathbf{H}_{t1}$ are considered as the first incident electromagnetic fields of the medium-coated conducting sphere, also described as $\mathbf{E}_{i2}$ and $\mathbf{H}_{i2}$, which can be expanded using spherical vector wave functions. They are [17,18]:

$$\mathbf{E}_{i2} = \sum_{nm}\left[\delta_{m,1} + \delta_{m,-1}\right]\left[a^{ix}_{nm}\mathbf{M}^{(1)}_{nm}(r, k_1) + b^{ix}_{nm}\mathbf{N}^{(1)}_{nm}(r, k_1)\right] \tag{8}$$

$$\mathbf{H}_{i2} = \frac{k_1}{i\omega\mu_1}\sum_{nm}\left[\delta_{m,1} + \delta_{m,-1}\right]\left[a^{ix}_{nm}\mathbf{M}^{(1)}_{nm}(r, k_1) + b^{ix}_{nm}\mathbf{N}^{(1)}_{nm}(r, k_1)\right] \tag{9}$$

where n is an integer valued from 0 to $+\infty$, while m is from $-n$ to n. The expansion coefficients in Equations (8) and (9) can be derived in [17,18]:

$$a^{ix}_{nm} = T\begin{cases} i^{n+1}\frac{2n+1}{2n(n+1)}, & m = 1 \\ i^{n+1}\frac{2n+1}{2}, & m = -1 \end{cases} \tag{10}$$

$$b_{nm}^{ix} = T\begin{cases} i^{n+1}\frac{2n+1}{2n(n+1)}, & m = 1 \\ -i^{n+1}\frac{2n+1}{2}, & m = -1 \end{cases} \tag{11}$$

$$\delta_{s,l} = \begin{cases} 1, & s = l \\ 0, & s \neq l \end{cases} \tag{12}$$

The spherical vector wave functions $\mathbf{M}_{nm}^{(l)}(\boldsymbol{r}, k)$, $\mathbf{N}_{nm}^{(l)}(\boldsymbol{r}, k)$ in Equations (8) and (9) can be shown in [4–18]:

$$\mathbf{M}_{mn}^{(l)}(r, k) = z_n^{(l)}(kr)\left[im\frac{P_n^m(\cos\theta)}{\sin\theta}e^{im\varphi}\,\hat{\theta} - \frac{dP_n^m}{d\theta}e^{im\varphi}\,\hat{\varphi}\right] \tag{13}$$

$$\mathbf{N}_{nm}^{(l)}(r, k) = n(n+1)\frac{z_n^{(l)}(kr)}{kr}P_n^m(\cos\theta)e^{im\varphi}\,\hat{r} + \frac{1}{kr}\frac{d(r z_n^{(l)}(kr))}{dr}\left[\frac{dP_n^m(\cos\theta)}{d\theta}\,\hat{\theta} + im\frac{P_n^m(\cos\theta)}{\sin\theta}\,\hat{\varphi}\right]e^{im\varphi} \tag{14}$$

where $z_n^{(l)}(x)$ denotes an appropriate kind of spherical Bessel function, while $j_n(x)$, $y_n(x)$, $h_n^{(1)}(x)$ and $h_n^{(2)}(x)$ are for l = 1, 2, 3 and 4, respectively. $P_n^m(x)$ denotes the associated Legendre function of degree n and index m.

The scattering electromagnetic fields of the first-incident electromagnetic fields from the medium-coated conducting sphere can be expressed as:

$$\mathbf{E}_{r2} = \sum_{nm}\left[A_{nm}^s\mathbf{M}_{nm}^{(3)}(r, k_1) + B_{nm}^s\mathbf{N}_{nm}^{(3)}(r, k_1)\right] \tag{15}$$

$$\mathbf{H}_{r2} = \frac{k_1}{i\omega\mu_1}\sum_{nm}\left[A_{nm}^s\mathbf{N}_{nm}^{(3)}(r, k_1) + B_{nm}^s\mathbf{M}_{nm}^{(3)}(r, k_1)\right] \tag{16}$$

Electromagnetic fields in the coated medium (region 2) can be expressed as following [18]:

$$\mathbf{E}_{st2} = \sum_{nm}\left[A_{nm}^{t2}\mathbf{M}_{nm}^{(1)}(r, k_2) + B_{nm}^{t2}\mathbf{N}_{nm}^{(1)}(r, k_2) + C_{nm}^{t2}\mathbf{M}_{nm}^{(2)}(r, k_2) + D_{nm}^{t2}\mathbf{N}_{nm}^{(2)}(r, k_2)\right] \tag{17}$$

$$\mathbf{H}_{st2} = \frac{k_2}{i\omega\mu_2}\sum_{nm}\left[A_{nm}^{t2}\mathbf{N}_{nm}^{(1)}(r, k_2) + B_{nm}^{t2}\mathbf{M}_{nm}^{(1)}(r, k_2) + C_{nm}^{t2}\mathbf{N}_{nm}^{(2)}(r, k_2) + D_{nm}^{t2}\mathbf{M}_{nm}^{(2)}(r, k_2)\right] \tag{18}$$

where in the inner and outer surface of the medium-coated conducting sphere, the tangential continuous boundary conditions are:

$$\begin{cases} \mathbf{E}_{i2}^t|_{r=r_2} + \mathbf{E}_{r2}^t|_{r=r_2} = \mathbf{E}_{st2}^t|_{r=r_2} \\ \mathbf{H}_{i2}^t|_{r=r_2} + \mathbf{H}_{r2}^t|_{r=r_2} = \mathbf{H}_{st2}^t|_{r=r_2} \end{cases} \tag{19}$$

$$\mathbf{E}_{st2}^t|_{r=r_1} = 0 \tag{20}$$

The superscript t is the tangential component of the electromagnetic fields, and we submit Equations (8), (9) and (15)–(18) to Equations (19) and (20) and applying the tangential orthogonality of spherical vector wave functions. The following six expressions can be derived:

$$[\delta_{m,1} + \delta_{m,-1}]a_{nm}^{ix}j_n(k_1r_2) + A_{nm}^s h_n^{(1)}(k_1r_2) = A_{nm}^{t2}j_n(k_2r_2) + C_{nm}^{t2}y_n(k_2r_2) \tag{21}$$

$$[\delta_{m,1} + \delta_{m,-1}]b_{nm}^{ix}R_n^{(1)}(k_1r_2) + B_{nm}^s R_n^{(3)}(k_1r_2) = B_{nm}^{t2}R_n^{(1)}(k_2r_2) + D_{nm}^{t2}R_n^{(2)}(k_2r_2) \tag{22}$$

$$\frac{k_1}{i\omega\mu_1}\left\{[\delta_{m,1} + \delta_{m,-1}]a_{nm}^{ix}R_n^{(1)}(k_1r_2) + A_{nm}^s R_n^{(3)}(k_1r_2)\right\} = \frac{k_2}{i\omega\mu_2}\left[A_{nm}^{t2}R_n^{(1)}(k_2r_2) + C_{nm}^{t2}R_n^{(2)}(k_2r_2)\right] \tag{23}$$

$$\frac{k_1}{i\omega\mu_1}\left\{[\delta_{m,1} + \delta_{m,-1}]b_{nm}^{ix}j_n(k_1r_2) + B_{nm}^s h_n^{(1)}(k_1r_2)\right\} = \frac{k_2}{i\omega\mu_2}\left[B_{nm}^{t2}j_n(k_2r_2) + C_{nm}^{t2}y_n(k_2r_2)\right] \tag{24}$$

$$A_{nm}^{t2}j_n(k_2r_1) + C_{nm}^{t2}y_n(k_2r_1) = 0 \tag{25}$$

$$B_{nm}^{t2}R_n^{(1)}(k_2r_1)+D_{nm}^{t2}R_n^{(2)}(k_2r_1)=0 \tag{26}$$

Then, the scattering coefficients in Equations (15) and (16) can be given:

$$A_{nm}^{s}=\frac{P_1R_n^{(1)}(k_1r_2)-wj_n(k_1r_2)}{wh_n^{(1)}(k_1r_2)-P_1R_n^{(3)}(k_2r_2)}a_{nm}^{ix}[\delta_{m,1}+\delta_{m,-1}] \tag{27}$$

$$\mathrm{B}_{\mathrm{nm}}^{\mathrm{s}}=\frac{\mathrm{P_1j_n(k_1r_2)-zR_n^{(1)}(k_1r_2)}}{\mathrm{zR_n^{(3)}(k_1r_2)-P_1h_n^{(1)}(k_1r_2)}}\mathrm{b_{nm}^{ix}}[\delta_{\mathrm{m},1}+\delta_{\mathrm{m},-1}] \tag{28}$$

where w and z are expressed as:

$$w=\frac{j_n(k_2r_1)R_n^{(2)}(k_2r_2)-y_n(k_2r_1)R_n^{(1)}(k_2r_2)}{j_n(k_2r_1)y_n(k_2r_2)-j_n(k_2r_2)y_n(k_2r_1)} \tag{29}$$

$$z=\frac{y_n(k_2r_2)R_n^{(1)}(k_2r_1)-j_n(k_2r_2)R_n^{(2)}(k_2r_1)}{R_n^{(1)}(k_2r_1)R_n^{(2)}(k_2r_2)-R_n^{(1)}(k_2r_2)R_n^{(2)}(k_2r_1)} \tag{30}$$

where P_1 and $R_n^{(l)}(kr)$ in Equations (27)–(30) are obtained as:

$$P_1=\sqrt{\frac{\varepsilon_1\mu_2}{\varepsilon_2\mu_1}} \tag{31}$$

$$R_n^{(l)}(kr)=\frac{1}{r}\frac{d}{dr}[rz_n^{(l)}(kr)] \tag{32}$$

The scattering electromagnetic fields of the buried medium-coated conducting sphere $\mathbf{E}_{r2}$ and $\mathbf{H}_{r2}$ in Equations (15) and (16) will be regarded as the second incident electromagnetic field to the plane (z = −d). By this incident electromagnetic field, on the basis of the image method [17–19], the reflected and transmitted electromagnetic fields from the plane z = −d can be expressed as follows:

$$\mathbf{E}_{r3}=\sum_{nm}\left[\mathrm{A_{nm}^{sr}}\mathbf{M}_{\mathrm{nm}}^{(3)}(\mathrm{r_{img}},\mathrm{k_1})+\mathrm{B_{nm}^{sr}}\mathbf{N}_{\mathrm{nm}}^{(3)}(\mathrm{r_{img}},\mathrm{k_1})\right] \tag{33}$$

$$\mathbf{H}_{r3}=\frac{\mathrm{k_1}}{\mathrm{i}\omega\mu_1}\sum_{nm}\left[\mathrm{A_{nm}^{sr}}\mathbf{N}_{\mathrm{nm}}^{(3)}(\mathrm{r_{img}},\mathrm{k_1})+\mathrm{B_{nm}^{sr}}\mathbf{M}_{\mathrm{nm}}^{(3)}(\mathrm{r_{img}},\mathrm{k_1})\right] \tag{34}$$

$$\mathbf{E}_{t3}=\sum_{nm}\left[\mathrm{A_{nm}^{st}}\mathbf{M}_{\mathrm{nm}}^{(3)}(\mathrm{r},\mathrm{k_0})+\mathrm{B_{nm}^{st}}\mathbf{N}_{\mathrm{nm}}^{(3)}(\mathrm{r},\mathrm{k_0})\right] \tag{35}$$

$$\mathbf{H}_{t3}=\frac{\mathrm{k_0}}{\mathrm{i}\omega\mu_0}\sum_{nm}\left[\mathrm{A_{nm}^{st}}\mathbf{N}_{\mathrm{nm}}^{(3)}(\mathrm{r},\mathrm{k_0})+\mathrm{B_{nm}^{st}}\mathbf{M}_{\mathrm{nm}}^{(3)}(\mathrm{r},\mathrm{k_0})\right] \tag{36}$$

Similar to [17–19], $\mathbf{E}_{t3}$ is presented by the global coordinate system, while $\mathbf{E}_{r3}$ is presented by the local coordinate system. The coordinate components of the global coordinate system are r, θ, and ϕ, and the coordinate components of the local coordinate system are r_{img}, θ_{img}, and ϕ_{img}. The relationship between the global coordinate system and the local coordinate system is shown in Figure 2.

The coefficients A_{nm}^{sr} and B_{nm}^{sr} can be obtained by applying the tangential continuous boundary condition of electromagnetic fields at point P in the plane boundary, which is shown in Figures 1 and 2, and then the reflected electric field in the local coordinated system can be transformed to the global coordinate system, and it can be written as:

$$\mathbf{E}_{r\,3'}=\sum_{nm}\left[\mathrm{C_{nm}^{sr}}\mathbf{M}_{\mathrm{nm}}^{(1)}(\mathrm{r},\ \mathrm{k_1})+\mathrm{D_{nm}^{sr}}\mathbf{N}_{\mathrm{nm}}^{(1)}(\mathrm{r},\mathrm{k_1})\right] \tag{37}$$

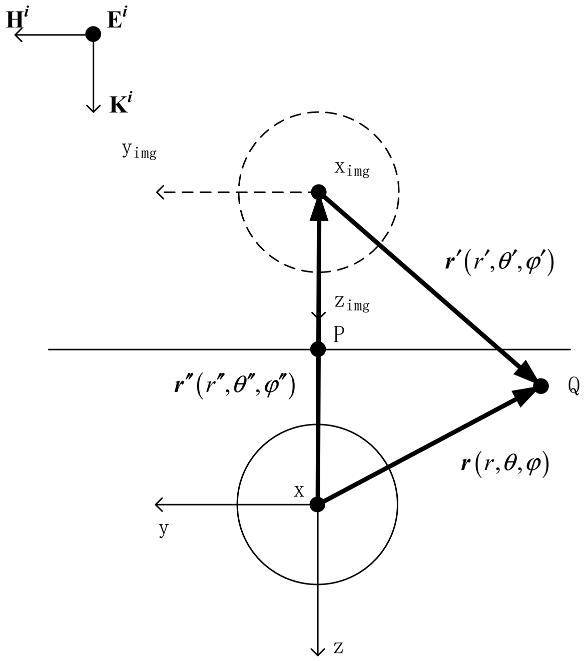

Figure 2. Relationship between r, r', r'' in the global coordinate system and local coordinate system.

According to the relationship of vectors in the addition theorem [20,21], the spherical vector wave functions are expanded as:

$$\mathbf{M}_{\mathrm{nm}}^{(1)}(\mathrm{r},\mathrm{k}_1)=\sum_{\mathrm{nm}}\left[\mathrm{A}_{\mathrm{nm,vu}}^{(1)}\mathbf{M}_{\mathrm{vu}}^{(1)}(\mathrm{r}',\mathrm{k}_1)+\mathrm{B}_{\mathrm{nm,vu}}^{(1)}\mathbf{N}_{\mathrm{vu}}^{(1)}(\mathrm{r}',\mathrm{k}_1)\right] \tag{38}$$

$$\mathbf{N}_{\mathrm{nm}}^{(1)}(\mathrm{r},\mathrm{k}_1)=\sum_{\mathrm{nm}}\left[\mathrm{A}_{\mathrm{nm,vu}}^{(1)}\mathbf{N}_{\mathrm{vu}}^{(1)}(\mathrm{r}',\mathrm{k}_1)+\mathrm{B}_{\mathrm{nm,vu}}^{(1)}\mathbf{M}_{\mathrm{vu}}^{(1)}(\mathrm{r}',\mathrm{k}_1)\right] \tag{39}$$

The coefficients C_{nm}^{sr} and D_{nm}^{sr} are derived by combining Equations (33) and (37)–(39), as the next expression is given:

$$\begin{bmatrix} \mathrm{C}_{\mathrm{nm}}^{\mathrm{sr}} & \mathrm{D}_{\mathrm{nm}}^{\mathrm{sr}} \end{bmatrix}\begin{bmatrix} \sum\limits_{\mathrm{vu}}[\mathbf{M}_{\mathrm{vu}}^{(1)}(\mathrm{r}',\mathrm{k}_1)\mathrm{A}_{\mathrm{nm,vu}}^{(1)}+\mathbf{N}_{\mathrm{vu}}^{(1)}(\mathrm{r}',\mathrm{k}_1)\mathrm{B}_{\mathrm{nm,vu}}^{(1)}] \\ \sum\limits_{\mathrm{vu}}[\mathbf{N}_{\mathrm{vu}}^{(1)}(\mathrm{r}',\mathrm{k}_1)\mathrm{A}_{\mathrm{nm,vu}}^{(1)}+\mathbf{M}_{\mathrm{vu}}^{(1)}(\mathrm{r}',\mathrm{k}_1)\mathrm{B}_{\mathrm{nm,vu}}^{(1)}] \end{bmatrix}=\begin{bmatrix} \mathrm{A}_{\mathrm{nm}}^{\mathrm{sr}} & \mathrm{B}_{\mathrm{nm}}^{\mathrm{sr}} \end{bmatrix}\begin{bmatrix} \mathbf{M}_{\mathrm{nm}}^{(3)}(\mathrm{r}',\mathrm{k}_1) \\ \mathbf{N}_{\mathrm{nm}}^{(3)}(\mathrm{r}',\mathrm{k}_1) \end{bmatrix} \tag{40}$$

where the initial values of the transform coefficients $A_{vu,nm}^{(1)}, B_{vu,nm}^{(1)}$ in Equations (38)–(40) and the recursive method are discussed in [20,21] in detail, and then the coordinate transformation coefficients $A_{vu,nm}^{(1)}, B_{vu,nm}^{(1)}$ are obtained. The reflected electromagnetic fields from the boundary plane will again act as the next incident electromagnetic fields to the buried medium-coated conducting sphere. We repeat Formulas (8)–(40) until the electric field at plane boundary point P has converged, since the scattering fields are much smaller than the incident fields according to electromagnetic scattering theory [2]. The electrical field at point P (in Figures 1 and 2) can be obtained as:

$$\mathbf{E}_p=\mathbf{E}_{i2}+\mathbf{E}_{r,q},\quad \mathrm{q}=2,\ 3,\ 4,\ldots \tag{41}$$

3. Numerical Results and Discussion

In the last section, the necessary theoretical formulas of the multiple electromagnetic scattering by a buried medium-coated conducting sphere are presented. To gain more physics insight into the problem, some numerical results in this section are calculated for the study of electromagnetic scattering by a buried medium-coated conducting sphere. The inner and outer radii of the medium-coated conducting sphere are r_1 and r_2, the depth of the buried medium-coated conduction sphere is d, and the relative permittivity of the buried medium and coated medium are $\varepsilon_{\mathrm{r}1}$ and $\varepsilon_{\mathrm{r}2}$. Some numerical results of the electric field at point P in the plane boundary are given using Fortran program, and the calculation results of software FEKO are also given in those figures. All the parameters are set as shown in Table 1 in detail. The simulation of frequency is set to 1 MHz–10 MHz on a note computer (CPU: Intel(R) Core (TM) i3-4030U with RAM is 4(GB)), since the application of electromagnetic scattering by buried objects is in microwave remote sensing, buried target detection, etc. Figures 3 and 4 are shown in this section. The relative error is targeted to those figures as:

$$\text{error} = \frac{|\mathbf{E}_{r,q}|}{|\mathbf{E}_p|} \times 100\% \tag{42}$$

where the $\mathbf{E}_{r,q}$ ($q \geq 2$) is shown in Equation (15) or Equation (33) and $\mathbf{E}_p$ is shown in Equation (41), the relative error is 0.5%, and the iteration number q in Equation (41) is 4 in Figure 3 and 3 in Figure 4, respectively, which shows that the present method of multiple scattering by a buried medium-coated conducting sphere is very effective.

Table 1. Different simulation cases for buried medium-coated conducting sphere.

Case #	ε_{r1}	σ_2 (S/m)	ε_{r2}	r_1 (m)	r_2 (m)	D (m)	Fortran-Time (s)	Feko-Time (h)
case 1	2	0	5	1	1.5	8	19.50	2.85
case 2	2	0	30	1	1.5	8	20.04	2.79
case 3	2	0	5	1	1.5	6	20.44	2.83

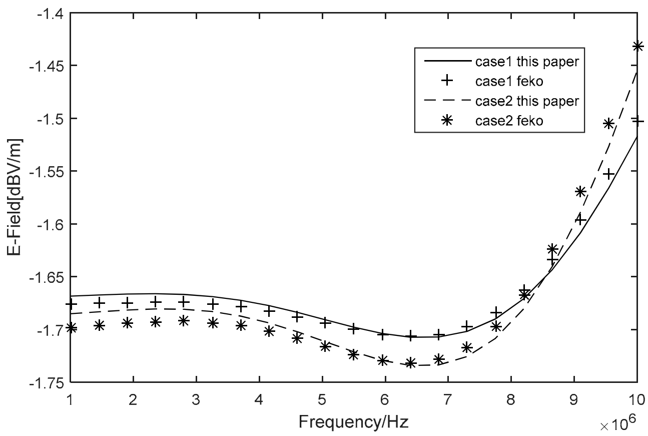

Figure 3. Electric field values with the frequency under different relative permittivities of the coating medium.

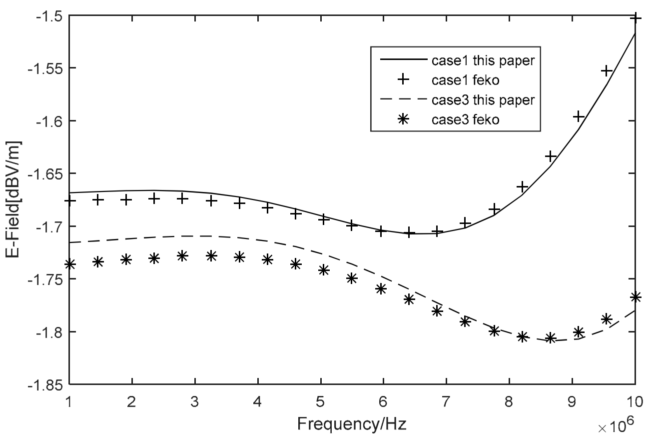

Figure 4. Electric field values with the frequency under different burial depths.

From Table 1, it can be seen that the present method takes much less time than the software FEKO, since the present method is an analytical solution.

Figure 3 shows the curve of the electric field value at point P as a function of frequency under the different relative permittivities of the coating medium. At a low frequency (1−8.3 MHz), the larger the relative permittivity of the coating medium, the smaller the electrical fields at point P, and at a high frequency (more than 8.3 MHz), the smaller the relative permittivity of the coating medium, the smaller the electrical fields at point P. This shows that the permittivity of the coating medium has different characterization, and the changeability of the electrical fields at point P is more complex.

Figure 4 shows the curve of the electric field value at point P as a function of frequency under different buried depths. In this figure, the electrical field value at point P decreases and then increases with the increase in frequency (case 1 and case 3), but it decreases slowly and then increases faster in case 1 than in case 3. The buried depth of the medium-coated conduction sphere reduces, and the electrical field at point P reduces; when the frequency is larger, the smaller the electrical field is at point P in case 3, which is different to the law: the larger the electrical size, the large the scattering fields, and as the buried depth reduces, the electrical field increases. In the detection of buried objects, this must be considered.

4. Conclusions

An analytical solution to the multiple electromagnetic scattering by a buried medium-coated conducting sphere is presented in this paper. Using an image method, the plane wave expanded in terms of spherical vector wave functions in isotropic medium, and applying an additive theorem of spherical vector wave functions to solve the coefficients of the transformation matrix and then transforming the vector field in the local coordinate system into the global coordinate system, the scattering electrical field at point P in the plane boundary by a buried medium-coated conducting sphere is derived. The initial values of the transformation matrix coefficients can be derived by traditional methods [20,21]. Some numerical results are given in the latter section of this paper, and those, compared with those of the FEKO software, coincide well enough. The present method has a definite advantage in terms of computing speed, and the analytical solution in this paper can be used in microwave remote sensing, buried target detection, wave propagation in terrestrial environments, etc.

Author Contributions: Formal analysis, C.Y. and Y.G.; funding acquisition and paper revision, P.Z.; software and data, L.W. All authors have read and agreed to the published version of the manuscript.

Funding: This research was funded by the National Natural Science Foundation of China under Grant 41842010.

Data Availability Statement: The authors confirm that the data supporting the findings of this study are available within the article.

Conflicts of Interest: The authors declare no conflict of interest.

References

1. Mie, G. Beitrage zur Optik truber Medien speziell Kolloidaller Metallosungen. *Ann. Der Phys.* **1908**, *25*, 337–455.
2. Brillouin, L. The Scattering Cross Section of Spheres for Electromagnetic Waves. *J. Appl. Phys.* **1949**, *20*, 1110–1125. [CrossRef]
3. Stratton, J.A. *Electromagnetic Theory*; McGraw-Hill: New York, NY, USA, 1941.
4. Batool, S.; Frezza, F.; Mangini, F.; Xu, Y.L. Scattering from multiple PEC sphere using Translation Addition Theorems for Spherical Vector Wave Function. *J. Quant. Spectrosc. Radiat. Transf.* **2020**, *248*, 106905. [CrossRef]
5. Frezza, F.; Mangini, F. Vectorial spherical-harmonics representation of an inhomogeneous elliptically polarized plane wave. *J. Opt. Soc. Am. A* **2015**, *32*, 1379–1383. [CrossRef] [PubMed]
6. Gao, C.; Sun, B.; Zhang, Y. Electromagnetic wave scattering by charged coated spheres. *J. Quant. Spectrosc. Radiat. Transf.* **2021**, *21*, 107757. [CrossRef]
7. Shore, R.A. Scattering of an Electromagnetic Linearly Polarized Plane Wave by a Multilayered Sphere: Obtaining a computational form of Mie coefficients for the scattered field. *IEEE Antennas Propag. Mag.* **2015**, *57*, 69–116. [CrossRef]
8. Batool, S.; Nisar, M.; Dinia, L.; Mangini, F.; Frezza, F. Multiple Scattering by Two PEC Spheres Using Translation Addition Theorem. *Electronocs* **2022**, *11*, 126. [CrossRef]
9. Tang, H.; Li, R.; Gong, S.; Wei, B.; Yang, L.; Zhu, Z.; Wu, Y.; Mitri, F.G. Scattering of a Arbitrary Optical Polarized Beams by a PEMC Sphere. *J. Quant. Spectrosc. Radiat. Transf.* **2022**, *281*, 108101. [CrossRef]

10. Raad, S.H.; Atlasbaf, Z. Scattering From Graphene-Based Multilayered Spherical Structures. *IEEE Trans. Nanotechnol.* **2019**, *18*, 1129–1136. [CrossRef]
11. Guo, L.; Shen, J. Internal and external-fields of a multilayered sphere illuminated by the shaped beam: Rescaled quantities for numerical calculation. *J. Quant. Spectrosc. Radiat. Transf.* **2020**, *250*, 107004. [CrossRef]
12. Wang, G.L.; Chew, W.C. Formal solution to the electromagnetic scattering by buried dielectric and metallic spheres. *Radio Sci.* **2004**, *39*, 1–17. [CrossRef]
13. Bellez, S.; Bourlier, C.; Kubicke, G. 3-D scattering from a PEC target buried beneath a dielectric rough surface: An efficient PILE-ACA algorithm for solving a hybrid KA-EFIE formulation. *IEEE Trans. Antennas Propag.* **2015**, *63*, 5003–5014. [CrossRef]
14. Frezza, F.; Mangini, F.; Tedeschi, N. Electromagnetic scattering by two concentric spheres buried in a stratified material. *J. Opt. Soc. Am. A* **2015**, *32*, 277–286. [CrossRef] [PubMed]
15. Frezza, F.; Mangini, F. Electromagnetic scattering by a buried sphere in a lossy medium of an inhomogeneous plane wave at arbitrary incidence: Spectral-domain method. *J. Opt. Soc. Am. A* **2016**, *33*, 947–953. [CrossRef] [PubMed]
16. Zamani, H.; Tavakoli, A.; Dehmollaian, M. Scattering by a Dielectric Sphere Buried in a Half-Space With a Slightly Rough Interface. *IEEE Trans. Antennas Propag.* **2018**, *66*, 347–359. [CrossRef]
17. Zhang, X.X.; Geng, Y.L.; Cheng, Z.Q. A Multiple-Reflection Solution to Electromagnetic Scattering by a Buried Sphere. *IEEE Trans. Antennas Propag.* **2020**, *68*, 3313–3317. [CrossRef]
18. Geng, Y.L.; Wu, L.J.; Zhang, P.Q. An Analytical Solution of Scattering by a Buried Two Concentric Sphere. In Proceedings of the 2020 Cross Strait Radio Science & Wireless Technology Conference, Fuzhou, China, 11–14 October 2020; pp. 1–2.
19. Nasr, M.A.; Eshrah, I.A.; Hashish, E.A. Electromagnetic scattering from a buried cylinder using a multiple reflection approach: TM Case. *IEEE Trans. Antennas Propag.* **2014**, *62*, 2702–2707. [CrossRef]
20. Gurel, L.; Chew, W.C. Scattering solution of three-dimensional array of patches using the recursive T-matrix algorithms. *IEEE Microw. Guided Wave Lett.* **1992**, *2*, 182–184. [CrossRef]
21. Wang, Y.M.; Chew, W.C. An efficient way to compute the vector addition theorem. In Proceedings of the IEEE Antennas and Propagation Society International Symposium, Ann Arbor, MI, USA, 28 June–2 July 1993; pp. 174–177.